NUMERICAL SIMULATION OF FLOW PATTERN INSIDE A POOL-AND-WEIR FISHWAY

S. Abdelaziz[1], M. D. Bui[1], K. Hayashida[2], and P. Rutschmann[1]

[1]Institute of Hydraulic and Water Resources Engineering, Technische Universität München - Germany
[2]Watershed Environmental Engineering Research Team, Civil Engineering Research Institute of Cold Region - Japan
E-mail: Shokry@bv.tum.de

Abstract

Over the past few years, numerical modeling has been used to study flow structure in pool-and-weir fishway. Such simulations can help to visualize the non-trivial flow patterns in fish ladders (Khan, 2006; Atsushi et al., 2009). However, there is still limited knowledge about effects of the length-to-depth ratio of a pool-and-weir fishway on the flow structure.

In this study, the commercial CFD code FLOW-3D is applied to simulate flows in a fish ladder. The purposes of this study are to advance our knowledge of fishway flow patterns and to provide a suitable guidance for an optimal design.

Experimental data archived from a previous study of Hayashida, et al., (2001) are used to calibrate and validate the numerical model. The result showed that the model is capable of simulating the flow pattern in the pool with acceptable accuracy. Further, the numerical model is applied to study effects of the ratio between the weir length and the pool depth on the flow structure in the fish ladder.

Introduction

One approach to study the fish movement through fish passes is to track its behavior against the change of hydraulic condition. This approach may allow us to assess the efficiencies of fishways and provide information of the proportions of the migrating populations that actually move upstream. Additionally, this approach can help us to better understand of the mentality of the fish for traversing a velocity barrier.

Monitoring the fish movement inside the fish passage can be used for calibration and validation of numerical model for fish movement in relation to different hydraulic conditions. Abdelaziz et al (2011) developed a model based on the concept of energy expenditure with random movements and turbulence effects to simulate the fish upstream movement inside the culvert, where the direction of flow was almost constant. This technique is not valid for the case, when the flow direction changes point by point e.g. in a pool-and-weir fishway. In this case, based on high water flow the fish recognizes the direction of the fishway. At the same time, the fish tries to minimize the energy expenditure by travelling against the lower velocities. Power et al (1985) suggested that the fishway entrance should site as close as possible to the source of the competing flow from the turbine. Another strategy suggested by Castro-Santos and Haro (2008) is to supplement the flow at the fishway entrance. This increases the ratio of flow at the fishway entrance to turbine flow without increasing the total flow passed through fishway itself.

Over the past few years, numerical models have been set up occasionally to depict flow structures. Such simulations can help to visualize the non-trivial flow patterns in fishway pools (Heimerl et al., 2008; Chorda et al., 2010; Xu, 2009). Most of these studies concentrated on Vertical Slot Fishway and very few studies focused in the pool and weir type (Atsushi, 2009).

In this study, numerical modeling was carried out to investigate the effects of changing the pool scale in a pool and weir fishway. The FLOW-3D computer program was applied to simulate the flow. The purposes of this study are to advance our knowledge of fishway flow patterns and to provide a suitable guidance for an optimal design.

Experimental Method

Hayashida, et al, (2001) have conducted experiments for the flow and fish movement inside a pool-and-weir fishway. The experiment was done in a two-dimensional water channel 60cm wide consisting of two weirs 20cm thick and one pool, where the pool length (L), the pool water depth (H), and shapes of weir can be changed. The head between the weirs and overflow water depth was fixed to 10cm throughout a series of the experiments. The swimming behaviors of Japanese daces by changing the scale of the pool and the shape of the weir were studied. Eight different cases were set out by changing the pool length (L) to 50, 100 and 200cms and the Weir heights (H) to 30/20, 60/50 and 90/80 cms. The grade of the fishway was determined by the pool length. Accordingly, the grade of the fishway is 1/7 for a pool length of 50cm, 1/12 for 100cm, and 1/22 for 200cm, respectively.

Numerical Approach

In the Program FLOW-3D, the hydrodynamic module is based on the solution of the three-dimensional Navier-Stokes equations and the continuity equation for incompressible flows. The governing equations can be written in a tensor form for a control volume as follows (Flow Science Inc., 2008):

$$\frac{\partial(u_i A_i)}{\partial x_i} = 0 \qquad (1)$$

$$\frac{\partial U_i}{\partial t} + \frac{1}{V_f}\left(U_j A_j \frac{\partial U_i}{\partial X_j}\right) = -\frac{1}{\rho}\frac{\partial P}{\partial X_i} + f_i \qquad (2)$$

where:

$$\rho V_f f_i = \tau_{b,i} - \left[\frac{\partial}{\partial X_j}\left(A_j S_{ij}\right)\right]; \quad S_{ij} = -\mu_{tot}\left[\frac{\partial U_i}{\partial X_j} + \frac{\partial U_j}{\partial X_i}\right] \qquad (3)$$

where U_i (1, 2, 3)= are the velocity components; P = pressure; A_i = fractional area open to flow in the i-direction; V_f = fractional volume open to flow; f_i = the gravity force per unit volume; S_{ij} = strain rate tensor; $\tau_{b,i}$ = wall shear stress; ρ = density of water; μ_{tot} = total dynamic viscosity, which includes the effects of turbulence ($\mu_{tot}=\mu+\mu_T$); μ = dynamic viscosity; and μ_T = eddy viscosity.

In FLOW3D, alternative schemes for turbulence closure, namely one-equation for turbulent energy k, standard k-ε, renormalization-group (RNG) k-ε, and large eddy simulation (LES) models, can be applied. The k-ε closure schemes will be considered in this paper, where the turbulent viscosity can be expressed as the product of the turbulent velocity and length scale. Therefore,

$$\mu_T = \frac{\rho C_\mu k^2}{\varepsilon} \qquad (4)$$

The closure equations for the turbulent kinetic energy k, and the dissipation rate ε, are given in a tensor form by:

$$\frac{\partial k}{\partial t} + \frac{1}{V_f} U_i A_i \frac{\partial k}{\partial X_i} = C_{sp}\frac{\mu}{\rho V_f}\left[2A_i\left(\frac{\partial U_i}{\partial X_i}\right)^2 + \left(\frac{\partial U_i}{\partial X_j} + \frac{\partial U_j}{\partial X_i}\right)\left(A_j \frac{\partial U_i}{\partial X_j} + A_i \frac{\partial U_j}{\partial X_i}\right)\right] - \frac{1}{V_f}\frac{\partial}{\partial X_j}\left[\frac{A_i}{\rho}\left(\mu + \frac{\mu_T}{\sigma_k}\right)\frac{\partial k}{\partial X_j}\right] \qquad (5)$$

where C_{sp} is an empirical factor called the shear production coefficient with default value=1.0

$$\frac{\partial \varepsilon}{\partial t} + \frac{1}{V_f} U_i A_{xi} \frac{\partial \varepsilon}{\partial x_i} = C_{\varepsilon 1}\frac{\varepsilon}{k}\left(C_{sp}\frac{\mu}{\rho V_f}\left(2A_{xi}\left(\frac{\partial U_i}{\partial X_i}\right)^2 + \left(\frac{\partial U_i}{\partial X_j} + \frac{\partial U_j}{\partial X_i}\right)\left(A_{xj} \frac{\partial U_i}{\partial X_j} + A_{xi} \frac{\partial U_j}{\partial X_i}\right)\right)\right) - \frac{1}{V_f}\frac{\partial}{\partial X_j}\left[\frac{A_{xi}}{\rho}\left(\mu + \frac{\mu_T}{\sigma_k}\right)\frac{\partial k}{\partial X_j}\right] - C_{\varepsilon 2}\frac{\varepsilon^2}{k} \qquad (6)$$

The closure coefficients and auxiliary relations in case of the standard k-ε model are: ($C_{\varepsilon 1}$= 1.44, $C_{\varepsilon 2}$ = 1.92, C_μ = 0.09, σ_k = 1.0, σ_ε = 1.3). The RNG approach is a mathematical technique that can be used to derive a turbulence model similar to the k- ε, results in a modified form of the ε equation which attempts to account for the different scales of motion through changes to the production term. The RNG model uses the same equations like k-ε model with different coefficients values ($C_{\varepsilon 1}$= 1.42, $C_{\varepsilon 2}$ is computed based on the values of k, ε and the shear rate, C_μ = 0.085, σ_k = 0.72, σ_ε = 0.72).

The wall boundary conditions are evaluated differently based on the chosen turbulence closure scheme. Transport turbulence closure scheme uses a law of the wall formulation. In FLOW3D the combined smooth and rough logarithmic law of the modified wall equation is iterated in order to solve for the shear velocity u* (Flow Science Inc., 2008):

$$u_o = u_*\left[\frac{1}{\kappa}\ln\left(\frac{\rho u_* y_o}{\mu + \rho a u_* k_s}\right) + 5.0\right] \qquad (7)$$

where κ = von Karman constant; a is a constant, which is equal to 0.247 for standard and RNG k-ε models; k_s = wall roughness; and y_0 = distance from the solid wall to the location of tangential velocity, u_0. The denominator of Eq. (8) represents an effective viscosity due to the effect of the rough boundary ($\mu_{eff}=\mu+\rho a u_* k_s$). If the cell is within the laminar sublayer (where $\rho u^* y_0/\mu \le 5.0$), the solution for the shear velocity is defined with:

$$u_* = \sqrt{\frac{\mu . u_o}{\rho y_o}} \qquad (8)$$

The solution for the shear velocity is used as the wall boundary conditions for the turbulent transport equations. At wall boundaries k and ε are defined with:

$$k = \frac{u_*^2}{\sqrt{C_\mu}}; \ \varepsilon = \frac{u_*^3}{\kappa y_o} \qquad (9)$$

Model calibration

The model was calibrated using the data for case-8 provided by Hayashida, et al., (2001). As shown in Fig.1, at the upstream and downstream boundary conditions the water elevations of 100cm and 80.13cm respectively were specified. The RNG turbulence model was used in this paper.

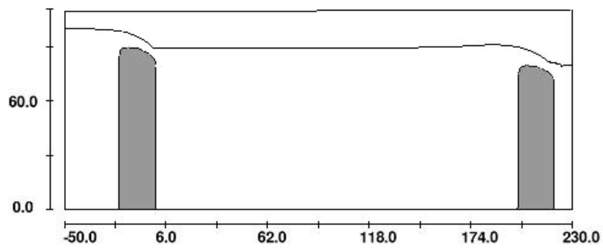

Figure 1: Model set up

In Fig.2 the simulated results were compared with the measurements of mean velocity in the domain. A good agreement between them has been achieved. In general, the velocity directions were ununiform, and a large area was occupied by low velocities. It can be seen that, in the experiment as well as in the numerical model the main flow was located in the domain near the wall and bed. The middle flow area is characterized by a circulated weak flow. On the other hand, the flow near the water surface is reversed due to the backwater effect. Fig.3 shows a comparison between the simulated maximum velocity paths and observations. The numerical model could simulate the water surface elevation and the maximum velocity path with a good accuracy, while very small difference can be seen in the domain near the water surface, where the flow takes place in the reversed direction. Fig. 4 presents the calculated and the measured maximum velocities near the bed. Again, a good agreement between calculation and measurement has been obtained.

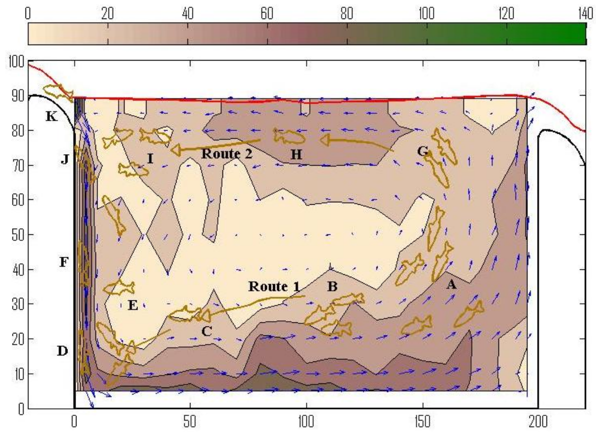

(a) Measured velocity distribution and swimming behavior (after Hayashida et al, 2001)

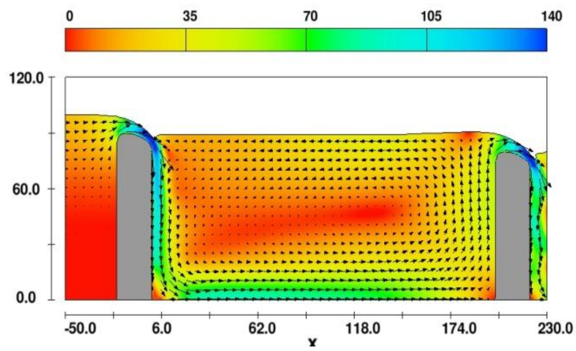

(b) Simulated velocity distribution

Figure 2: Mean flow pattern inside the pool tank.

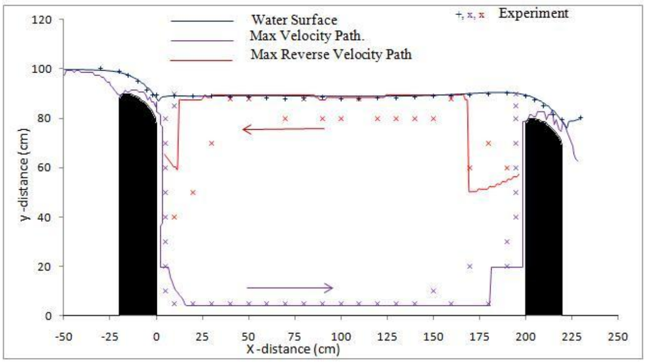

Figure 3: Maximum velocity paths inside the pool tank.

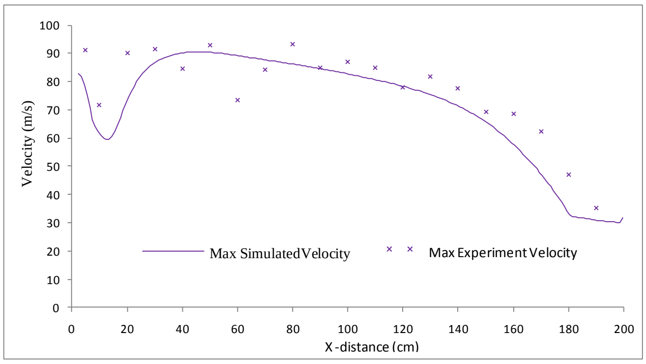

Figure 4: Maximum velocity near the bed.

Hayashida (2001) noticed that the fish stayed in the domain, where the velocity is slow and the current direction was constant. Most of the fish follow route 2 as indicated in Fig. 2-a. It was also noticed that the fish try to avoid the circulated flow inside the middle section of the pool, where the direction of flow is not clear.

Model Application

Hayashida et al, (2001) studied the swimming behavior of Japanese daces by changing the pool scale. Eight experiments were studied and the climbing frequency (the number of times that fish climb up the upstream weir) for each case was shown in Fig. 5. Finally, he classified the eight experiments to three levels according to the climbing frequency as **Level 1**: the most climbing frequency; **Level 2**: a lesser climbing frequency; and **Level 3**: a least climbing frequency

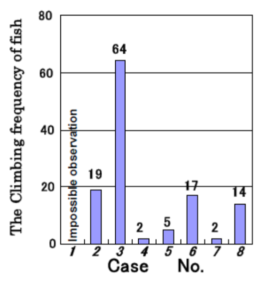

Figure 5: Climbing frequency of each case (after Hayashida et al, 2001)

In order to understand the fish movement inside the pool tank, the effect of changing the pool scale were studied using FLOW-3D program for the flow simulation and combining with the observations of fish movement given by Hayashida. Fig. 6 shows the simulated velocity distribution for case 3 as indicator for **Level 1** (the most climbing frequency). In this case, the pool length (L) was 200cm and the weir height (H) was 30cm for the upstream weir and 20 cm for the downstream weir. The calculated results show that in this case the flow has almost the same characteristic direction as flow directions for other cases. However, the circulation can be seen only in the upper part of the pool. This circulation vanishes in the middle of the tank and the flow becomes almost uniform and relatively slow.

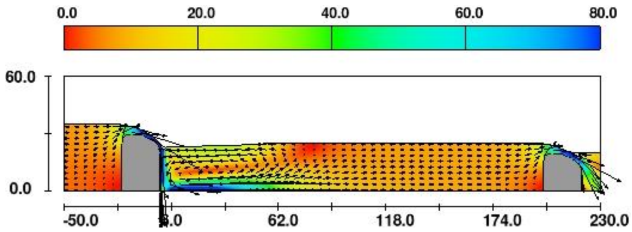

Figure 6: simulated flow pattern inside the pool tank for case 3 (**Level 1**).

Fig. 7 shows the simulated velocity distribution for case 4 as indicator for **Level 3** (a least climbing frequency). In this case, the pool length (L) was 100cm and the weir height (H) was 60cm for the upstream weir and 50 cm for the downstream weir. In this case, the flow field is characterized by the nonuniform flow direction. The main flow concentrates in the narrow area near the wall and bed while a large circulated flow in the middle area can be seen. Based on Hayashida's results, the fish follow one of the following three paths according to the flow pattern inside the pool: **Route 1**: Fish swim against the maximum flow direction; **Route 2**: Fish move in the a range of the bottom layer to the middle layer where the velocity is slow and the current direction was constant; and **Route 3**: Fish move toward the upstream weir in the neighborhood of the surface.

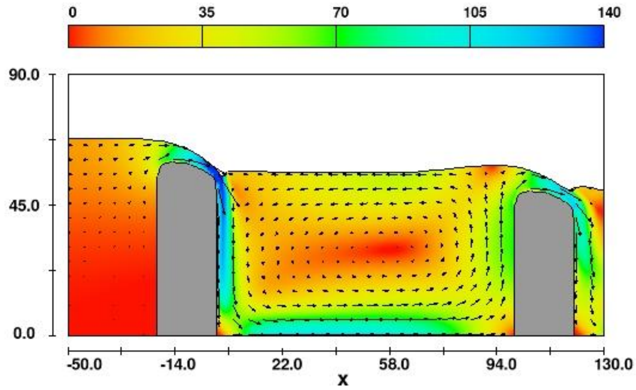

Figure 7: simulated flow pattern inside the pool tank for case 4 (**Level 3**).

Flow pattern in case 3 could be ideal for fish as the flow is almost uniform with small velocity. The fish follow the route 3, where the path is short. In all other cases, the water flow patterns are non-uniform. Since the fish are not familiar with pool tank, they try to follow the high flow direction to recognize the upstream direction. At the same time the fish try to minimize the energy by traveling against the low flow near the recognized direction. This idea is suitable for case 8, where fish following the route 2. If in the neighbor area the flow is characterized with changeable flow direction, the fish are bushed to follow the high flow direction in the route 1 (Case4).

Conclusion

The flow inside a pool-and-weir fishway was studied using an existing 3D numerical model (FLOW-3D). The model provided good results of flow pattern comparing to the experiment data given by Hayashida (2001). The calculated results showed that the flow inside the pool was highly non-uniform and a large area was occupied by a low velocity current. The dimension of the pool has a great effect on the distribution of flow in the pool. When the pool length is long and the weir height is small, the flow is mostly uniform. This flow condition could be perfect for Japanese daces which showed the most climbing frequency. By increasing the pool depth the flow non-uniformity becomes more intensively and accordingly, a climbing frequency can be reduced. By decreasing the pool length, the strong circulation of the flow can cause a very bad condition for the fish climbing ability.

References

Abdelaziz, S., Jhanwar, R., Bui, M.D., & Rutschmann, P., (2011). A Numerical Model for Fish Movement Through Culverts. 34th IAHR World Congress.

Atsushi, M. (2009). Studies on Design of Pool-and-Weir Type Fishway Focusing Flow Structure in the Fishway. Institute for Rural Engineering Report No. 49 (In japan)

Castro-Santos, T. & Haro, A. (2008). Fish Guidance and Passage at Barriers. Chapter 4 In "Fish Locomotion: An Etho-Ecological Approach. (P. Domenici and R. W. Blake, Ed.),Science Publishers, Enfield, NH.

Chorda, J. , Maubourguet, M., Roux, H., Larinier, M., Tarrade, L., & David, L. (2010). Two-Dimensional Free Surface Flow Numerical Model for Vertical Slot Fishways. J. of Hydraulic Research Vol. 48, No. 2 (2010), pp. 141–151

Flow Science, Inc. 2008: FLOW-3D User’s Manual. Flow Science, Inc.

Hayashida, k., Honda, T., Kayaba, Y., & Shimatani , Y. (2001). Flow Pattern of Pool-and-Weir Fishways inside the Pool and the Swimming Behaviors of Japanese Daces in the Fishways, Fish TREC-2001

Heimerl, S., Hagmeyer, M., & Echteler, C. (2008). Numerical Flow Simulation of Pool-Type Fishway: New Ways with Well-Known Tools. Hydrobiologia 609:189-196.

Khan, L. A. (2006). A Three-Dimensional Computational Fluid Dynamics (CFD) Model Analysis of Free Surface Hydrodynamics and Fish Passage Energetics in a Vertical-Slot Fishway. North American Journal of Fisheries Management, Vol.26, Issue 2, p. 255-267

Powers, P. D., Orsborn, J. F., Bumstead, T. W., Klinger-Kingsley, S. & Mih, W. C. (1985). Fishways: an Assessment of their Development and Design. Bonneville Power Administration, DOE/BP-36523-4, Portland, Oregon.

Xu, Tibing (2009). Numerical Simulation of Flow Structure in a Vertical Slot Fishway. 33rd IAHR Congress